Mapping two-way grids onto free-form surfaces

P. Winslow
Department of Engineering
University of Cambridge
Cambridge, UK

S. Pellegrino
Department of Engineering
University of Cambridge
Cambridge, UK

S.B. Sharma
SMART
Buro Happold
Bath, UK

Abstract

This paper presents a novel approach for the synthesis of single-layer grid structures, with a node connectivity of four, on free-form surfaces. Iterative structural analyses are used to make a more informed selection of the geometry of the grid structure. Central to this proposed approach is the parameterisation of the grid structure in terms of rod angles and spacing which, along with a process of homogenisation, facilitates multiobjective optimisation. This approach is demonstrated by taking an example free-form dome surface and evolving a set of grid designs, in order to minimise deflection under snow load and maximise buckling load; performance enhancements of 35-45% are achieved over 100 generations. A trade-off curve of potential solutions is generated from which a final grid structure can be chosen by the designer.

Keywords: design, free-form geometry, gridshell, homogenisation, multiobjective optimisation

1. Introduction

The advent of free-form 3-D modeling software has allowed architects and designers to create almost any shape imaginable. In order to physically realise these computer models, say as a building or a sculpture, an internal armature can be used along with non-load bearing panels to create the required external surface. Examples include Gehry's Guggenheim Museum in Bilbao and the Body Zone in the Millennium Dome, London . Use of a grid structure, consisting of a lattice of rods (see Figure 1) may be more desirable due to the potential for reductions in material usage and increased internal space. However, it is not always obvious how to create an efficient grid structure on a given architectural surface form.

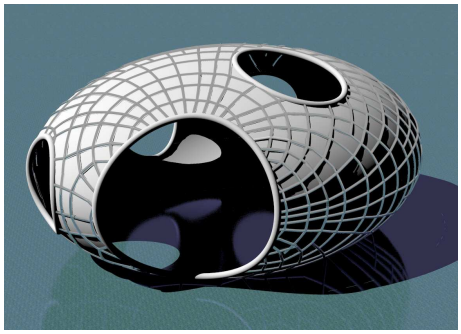

Fig. 1: Principal stress grid on a free-form surface.

A need for development of new computational structural engineering tools that can be applied to complex geometries has been explained by several authors [1, 2] . Mapping and processing of grid structures with complex geometry are problems frequently encountered by Buro Happold, however existing tools and techniques focus on relatively simple geometrical rules and algorithms to map a grid onto the surface. This paper will present a novel approach for synthesis of grid structures on free-form surfaces, utilising iterative structural analyses to make a more informed selection of structural geometry. The final aim of this approach is to create single-layer grid structures with a

node connectivity of four, i.e. rods define edges of quadrilaterals, as shown in Figure 1 and often referred to as a 'gridshell'.

2. Mapping Scheme

The grid synthesis approach that follows was inspired by recent research in advanced composite structures for aerospace applications. There is an obvious analogy between rods in a grid structure and fibres in a reinforced polymer composite; both lie on a chosen surface, and the direction of rod/fibre paths can be varied spatially. The rod/fibre direction in one region of the chosen surface could be very different to the directions elsewhere, thus the strength and stiffness of the structure can be tailored to meet a chosen set of objectives e.g. minimise mass, maximize stiffness, maximize buckling load etc. Analytical techniqies for "tow placement" in advanced composite structures has been described by Gurdal [3] and Setoodeh [4].

The flow chart in Figure 2 outlines the proposed method for synthesis of optimal grid structures, and the subsections that follow give further explanation. More details will be published elsewhere.

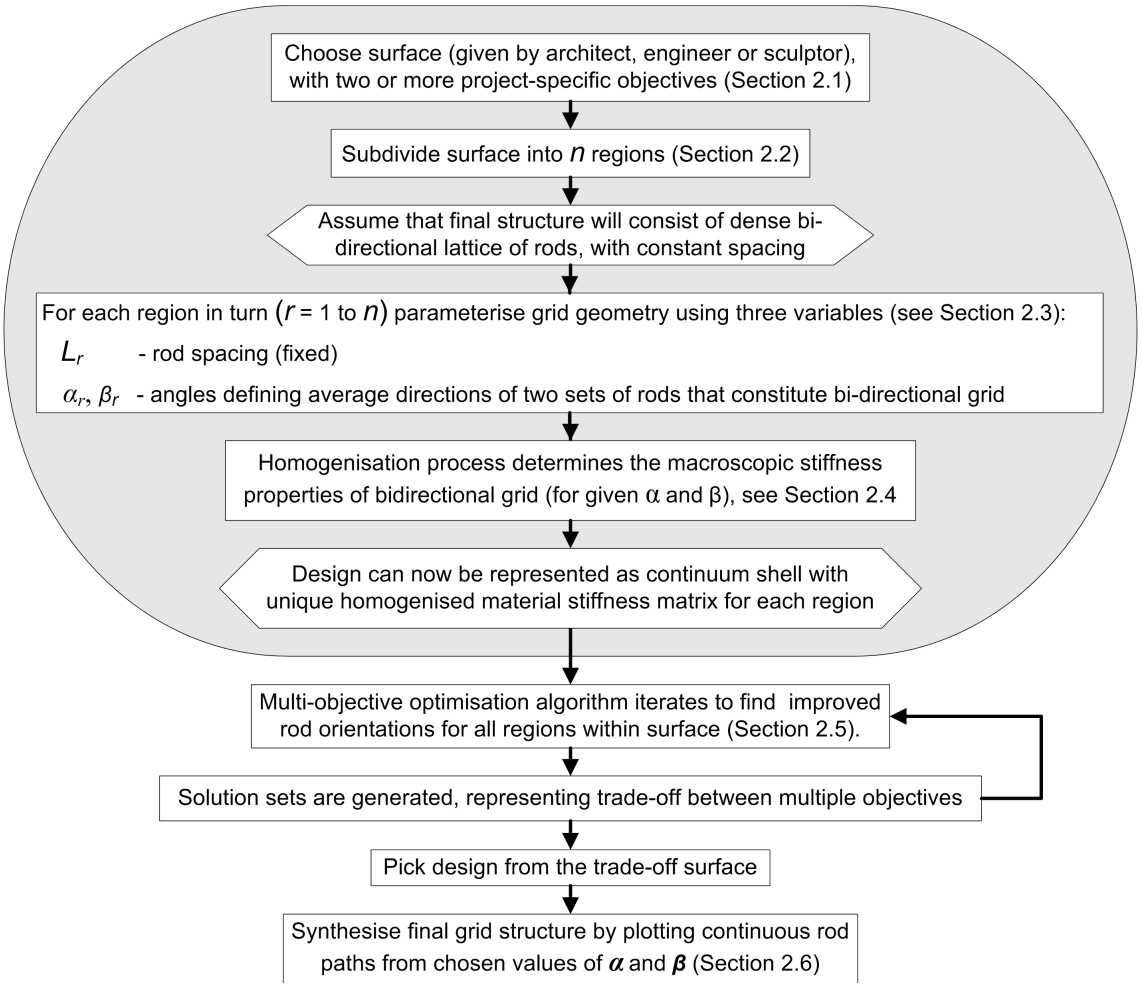

Fig. 2: Process overview.

2.1 Initialisation

We assume that the surface geometry is fixed. It could be a physical model, a point cloud (e.g. from a physical model using a digital probe) or a 3D surface created in a commercial CAD package. For the purposes of this paper it has been assumed that the surface geometry is represented using a NURBS

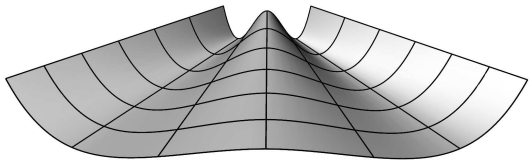

Fig. 3: NURBS surface subdivided with isoparametric lines.

(Non-Uniform Rational B-Spline) surface with *u,v* parameterisation. In order to synthesise a grid design it is clearly necessary to determine the project-specific objectives before progressing further. These could include serviceability criteria (e.g. deflection under self weight), dynamic requirements (maximising the fundamental frequency), minimising the maximum member forces under snow and or wind loading, etc.. For grid shell type structures global buckling is a major design consideration [2, 5]. Whilst a full non-linear analysis would be required in order to determine buckling behaviour accurately, an eigenvalue buckling analysis can be carried out much more rapidly and would be suitable for initial design synthesis and selection. Hence the latter method will be used throughout this paper.

2.2 Subdivision

The surface is spilt up into a number of regions, and each region is sized such that it is relatively flat and undistorted. This subdivision should also be relatively coarse in comparison to the rod spacing, *L*, that is to be realised in the final grid structure. Both of these attributes are crucial in ensuring accuracy of the homogenisation process. There are many possible ways in which the surface could be subdivided, but for the purposes of this paper it is carried out using uniformly spaced isoparametric lines. There are two compelling reasons for this approach:

1. The parameterisation of a NURBS surface is closely linked to the knot positions, and knots are closely linked to the distribution of control points over the surface. Control points are used to effect local changes in surface geometry and curvature, hence the regions will be smaller where the surface curvature is changing rapidly. In this way, each region created by isoparametric lines will be relatively undistorted.

2. Isoparametric lines are straightforward to create in many commercial 3D modelling packages, so specialist subdivision algorithms are not required.

2.3 Parameterisation

It will be assumed, at least initially, that the perpendicular spacing between rods, *L*, is constant (see Figure 4). The final grid structure will have a relatively dense lattice of rods such that:

$$L^2 \ll \text{area of region} \tag{1}$$

The grid geometry within each region can now be represented in terms of two variables:

1. α, half the average angle between the two sets of rods (see Figure 4).

2. β, relative in-plane rotation between the the local coordinate system for the region in question (x_r, y_r) and the grid coordinate axes (x, y).

In this way the fundamental properties of a grid design can be captured without the need to determine the coordinates for every single node; only two parameters are needed to specify the key load carrying directions in a bi-directional grid. The lengthy and difficult task of calculating the geometry for every node and rod can be avoided.

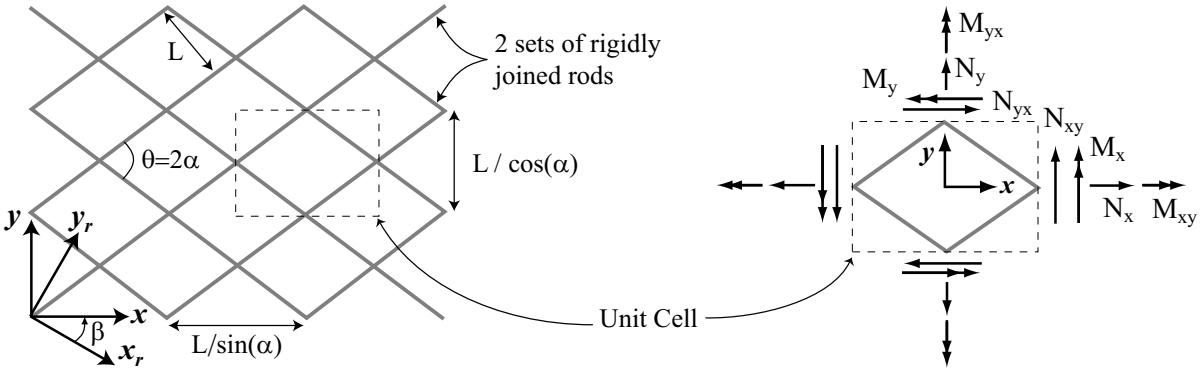

Fig. 4: Unit cell model for a regular grid of rigidly joined rods.

2.4 Homogenisation

The parameterisation of the grid geometry described in Section 2.3 is completed by replacing the grid with a continuum plate of equivalent stiffness. Therefore a scheme is required to find the stiffness matrix for this homogenised plate, as a function of the geometrical parameters α and β. This matrix will give the stress resultants $(N_x, N_y, N_{xy})^T$ and bending/twisting moments per unit length $(M_x, M_y, M_{xy})^T$ in terms of mid-plane strains $(\varepsilon_x^0, \varepsilon_y^0, \varepsilon_{xy}^0)^T$ and curvatures $(\kappa_x, \kappa_y, \kappa_{xy})^T$ for the homogenised plate:

$$\begin{bmatrix} N_x \\ N_y \\ N_{xy} \\ M_x \\ M_y \\ M_{xy} \end{bmatrix} = \begin{bmatrix} A_{11} & A_{12} & A_{16} & B_{11} & B_{12} & B_{16} \\ A_{21} & A_{22} & A_{26} & B_{21} & B_{22} & B_{26} \\ A_{61} & A_{62} & A_{66} & B_{61} & B_{62} & B_{66} \\ B_{11} & B_{12} & B_{16} & D_{11} & D_{12} & D_{16} \\ B_{21} & B_{22} & B_{26} & D_{21} & D_{22} & D_{26} \\ B_{61} & B_{62} & B_{66} & D_{61} & D_{62} & D_{66} \end{bmatrix} \begin{bmatrix} \varepsilon_x^0 \\ \varepsilon_y^0 \\ \varepsilon_{xy}^0 \\ \kappa_x \\ \kappa_y \\ \kappa_{xy} \end{bmatrix} \tag{2}$$

It is achieved by calculating the stiffness of a grid unit cell (Figure 4), which is subjected to periodic boundary conditions and Kirchhoff's thin plate assumption. The periodic boundary condition procedure described by Kueh [6] is followed, to calculate the coefficients of the ABD matrix. This involves imposing six unit deformations on the unit cell, in six different finite element analyses. Virtual work is then used to calculate the coefficients A_{11} to D_{66} in Equation 2.

The grid geometry is assumed to be planar, as shown in Figure 4. Therefore even before the numerics are implemented it is clear that there can be no coupling between stretching and bending effects, i.e. $B_{nm} = 0$, due to symmetry. In addition $A_{16} = A_{26} = D_{16} = D_{26} = 0$ (c.f. balanced symmetric layup in laminated plates). This may not be true in all practicable grid structures, however the general homogenisation technique described in this section is always applicable.

Figure 5 shows stiffness matrix coefficients for a sample grid constructed from steel tubes. The tubes are 60.3 mm in diameter, have 4 mm wall thickness and a spacing of L = 0.2 m.

2.5 Optimisation

A general optimisation problem can be stated as follows: find a set of design variables $\mathbf{x}$ which minimise the objective function $f(\mathbf{x})$ subject to a set of constraints. However, many real-world design problems require the simultaneous optimisation of (and trade off between) several performance measures e.g. deflection under self-weight, stress under snow load, buckling load etc.. There are a number of different approaches to such problems; constructing a composite objective function is a well known example. The drawback with these classical methods is that only a single design from the trade off surface is identified, and this point is heavily dependent upon the weightings chosen in the composite objective function.

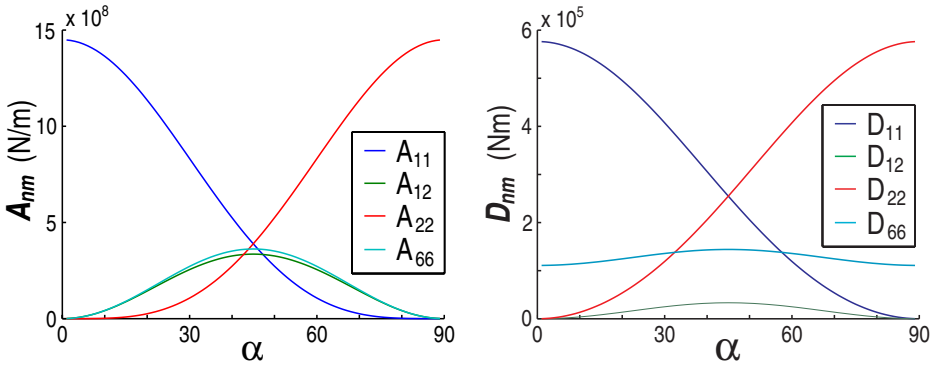

(a) A matrix (b) D matrix

Fig. 5: Coefficients of ABD matrix for sample grid

Stochastic optimisation methods [7] can be employed to evolve a large number of designs simultaneously, and this will give the trade-off surface for a multi-objective problem. The final design solution can then be picked from anywhere on this trade-off surface; the designer/engineer/architect thus retains a large degree of design freedom. A set of multiobjective evolutionary algorithms [8] are used in the present research and an overview of the procedure is shown in Figure 6. Whilst mutation and crossover are relatively well known, standard operators, it is the process for choosing suitable 'parents' which is central to multiobjective evolution.

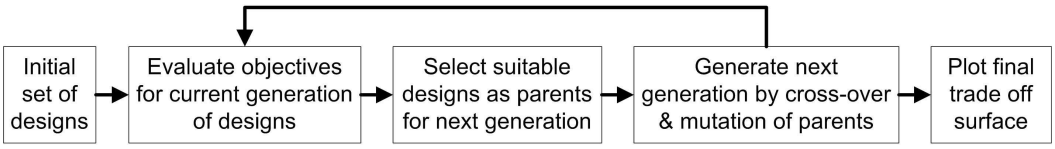

Fig. 6: Multiobjective evolutionary algorithm.

For the approach defined in this paper:
Minimise

$$f_1(\boldsymbol{\alpha}, \boldsymbol{\beta}), f_2(\boldsymbol{\alpha}, \boldsymbol{\beta}).....f_n(\boldsymbol{\alpha}, \boldsymbol{\beta}) \tag{3}$$

subject to

$$(0+\sigma) < \alpha_i < (90-\sigma) \tag{4}$$

$$0 < \beta_i < 180 \tag{5}$$

A small offset, σ, is necessary to prevent the ABD from becoming singular (which would happen as $\alpha \rightarrow 0$ or $\alpha \rightarrow 180$). Careful inspection of the unit cell geometry reveals that the design domain is actually covered twice when these ranges are used for α and β. However, it means that α and β remain independent variables, and the design space is continuous apart from the unavoidable transition between $\beta = 180$ and $\beta = 0$. This is due the unit cell geometry having rotational symmetry of order two (for all values of α).

2.6 Synthesis of grid geometry

Once the optimisation has been carried out a single design (i.e. a set of design variables) is picked from the trade-off surface. In order to synthesise the complete grid geometry, continuous rod paths must be plotted from the the design variables. Each path is plotted in a stepwise manner, using a weighted average of the optimum rod angles at the the nearest m regions, as shown in Figure 7. A

value of $m = 4$ is typically used; the rod plotting process is therefore a local scheme which can be successfully carried out on any surface.

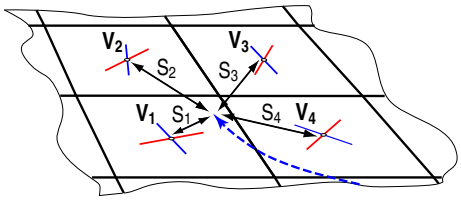

Fig. 7: Rod plotting by interpolation of four nearest regions. Dashed blue line indicates a continuous rod path. *Step direction* $= \sum_{i=1}^{4} \mathbf{V}_i / s_i$

3. Implementation

The algorithm described above has been implemented by creation of a bespoke C++ program to interface between the finite element program ANSYS and the PISA optimisation routines. Further processing of the results is carried out in Matlab.

4. Example: Free Form Dome

The method proposed in Sections 2 and 3 has been applied to the example surface shown in Figure 8 and the problem specified in Table 1. This free-form dome was created as a NURBS surface in Rhinoceros, a commercial CAD package, and has only one plane of symmetry. The boundary is restrained against translation in all directions and it is approximately 60 m long by 30 m wide, so it would be a suitable exhibition hall roof. The grid will be constructed from a standard size of steel tube, which will be spaced at 2 m centres. Typical loading for such a roof would be a uniformly distributed 1 kPa snow load, and the design should meet a serviceability criterion and an ultimate state criterion. Vertical deflection under snow load and the load factor required for global buckling will be used respectively; these quantities therefore become the two objectives for the optimisation.

The surface is subdivided into 25 regions using isoparametric lines (created automatically in Rhinoceros), and this would normally require the design variables to be $\alpha_1, \alpha_2, ...\alpha_{25}$ and $\beta_1, \beta_2, ...\beta_{25}$. However, only 24 design variables are needed to represent each grid design, due to symmetry and due to a more advanced parameter smoothing process.

The multi-objective evolutionary algorithm is initiated by randomly generating five hundred sets of design variables, with each set representing a possible grid design; this forms generation number one. The objectives are evaluated for every design, using ANSYS finite element program. The most promising of these designs, i.e. the ones with the smallest deflection under snow load and/or the highest buckling load, will be chosen as 'parents' from which the next generation is created by

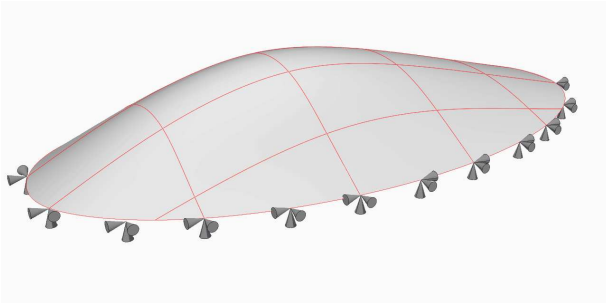

Fig. 8: Initial surface, with subdivisions and boundary conditions.

Table 1: Problem specification.

Loading	1 kPa pressure loading
Number of regions	25
Number of design variables	24 (by symmetry arguments)
Number of designs per generation	500
Number of generations	100
Rod data	Steel tube, ϕ169.3 mm, t = 10 mm
L	2 m
Objectives	Max. vertical deflection, buckling load factor

mutation and cross-over. The objectives are evaluated for every design in the new generation, and this whole process is repeated for as many generations as is desired.

The values of the objective functions at a number of stages in the evolution process are shown in Figure 9. The huge spread of the initial population makes it difficult to compare with other generations in a quantitative manner. However, it is clear that designs in later generations perform significantly better than designs in earlier generations. For instance, the vertical deflection of the best designs in generation 100 is about 45% less than the vertical deflection of the best designs in the initial population. The corresponding increase in buckling load is approximately 35%.

The trade-off curve has split into two parts at the 100th generation, which suggests that two forms/categories of design solutions are being generated. However, there is still a considerable range of different designs from which one could choose; the 100th generation now consists of two smaller trade-off curves but it has not converged to a single point. The arrows in Figure 9 show the location of two possible final designs which are selected from the 100th generation. Continuous rod paths are then plotted from the chosen design variables, as described in Section 2.6, and the complete grid geometries are shown in Figure 10. The first solution deflects 11 mm under the snow loading and buckles under a uniformly distributed load of 9.6 kN/m^2, whilst the second solution deflects 26 mm and buckles at 17.5 kN/m^2. Thus each structure has clear performance benefits, and the final choice of design can rest with the project architect and engineer.

5. Conclusions and further work

A new tool for synthesis of two-way grid structures has been presented. Central to this proposed tool is the parameterisation of the grid structure in terms of rod angles and spacing which, along with a process of homogenisation, facilitates multiobjective optimisation.

The example given in this paper shows promising preliminary results for the proposed design method; the prospective final designs presented can be inspected visually and both appear as sensible and rational solutions to carry the applied load. Evolving the design through 100 generations gives improvements in the first objective (deflection under snow loading) of approximately 45% and the second objective (buckling load) by approximately 35%. The multi-objective optimisation approach has successfully enabled a set of feasible structures to be created thus, unlike some other optimisation tools, design freedom is not significantly restricted.

Detailed comparisons between the final homogenised structures and the final discrete rod structures are currently underway. Further work will also include investigation of a local buckling failure criterion using stress resultants from the continuum analysis.

6. Acknowledgments

The authors would like to thank Buro Happold and the Engineering and Physical Sciences Research Council for financially supporting this project.

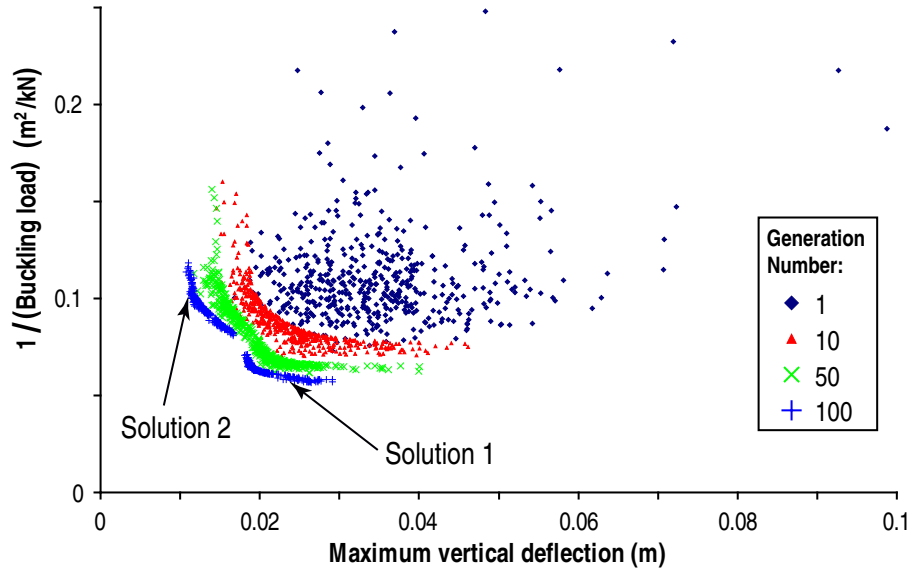

Fig. 9: Trade-off surface.

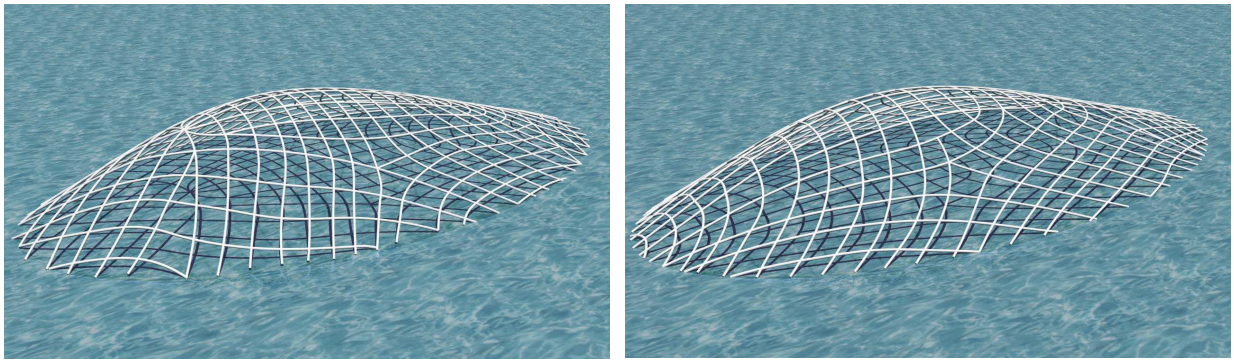

(a) Example Solution 1 (b) Example Solution 2

Fig. 10: Two designs chosen from 100th generation.

References

[1]. Luebkeman, C. *Computational design and optimization in building practice*, Arup Journal 3/2005, pp17-21

[2]. Schlaich, J. *New trade fair in Milan - Grid Topology and Structural behaviour of a free-formed glass-covered surface*, Int. Journal of Space Structures vol. 20, No. 1,2005

[3]. Gurdal, Z. and Olmedo, R. *In-plane response of laminates with spatially varying fiber orientations. Variable stiffness concept*, AIAA Journal, vol. 31 no. 4,1993, pp.751-758,

[4]. Setoodeh, S. and Abdalla, M.M. and Gurdal, Z. *Design of variable-stiffness laminates using lamination parameters*, Composites Part B: Engineering Vol. 37/4-5, 2006, pp301-309

[5]. Happold, E., Liddell, W.I. *Timber lattice roof for the Mannheim Budesgartenshau*, The Structural Engineer, 53/3, March 1975, pp99-135,

[6]. Kueh, A. and Pellegrino, S. ABD Matrix of Single-Ply Triaxial Weave Fabric Composites, American Institute of Aeronautics and Astronautics SDM Conference 2007

[7]. Reeves, C.R. *Modern heuristic techniques for combinatorial problems*, McGraw-Hill 1995

[8]. *Platform Independent Interface for Search Algorithms (PISA)*, Swiss Federal Institute of Technology, Zurich.